Published in final edited form as:
Acta Biomater. 2014 November ; 10(11): 4574–4582. doi:10.1016/j.actbio.2014.07.011.

Synthetic biodegradable hydrogel delivery of demineralized bone matrix for bone augmentation in a rat model

Lucas A. Kinard[1], **Rebecca L. Dahlin**[2], **Johnny Lam**[2], **Steven Lu**[2], **Esther J. Lee**[2], **F. Kurtis Kasper**[2], and **Antonios G. Mikos**[1,2,*]

[1]Rice University, Department of Chemical and Biomolecular Engineering

[2]Rice University, Department of Bioengineering

Abstract

There exists a strong clinical need for a more capable and robust method to achieve bone augmentation, and a system with fine-tuned delivery of demineralized bone matrix (DBM) has potential to meet that need. As such, the objective of the present study was to investigate a synthetic biodegradable hydrogel for the delivery of DBM for bone augmentation in a rat model. Oligo(poly(ethylene glycol) fumarate) (OPF) constructs were designed and fabricated by varying the content of rat-derived DBM particles (either 1:3, 1:1, or 3:1 DBM:OPF weight ratio on a dry basis) and using two DBM particle size ranges (50–150 or 150–250 μm). The physical properties of the constructs and the bioactivity of the DBM were evaluated. Select formulations (1:1 and 3:1 with 50–150 μm DBM) were evaluated *in vivo* compared to an empty control to investigate the effect of DBM dose and construct properties on bone augmentation. Overall, 3:1 constructs with higher DBM content achieved the greatest volume of bone augmentation exceeding 1:1 constructs and empty implants by 3-fold and 5-fold, respectively. As such, we have established that a synthetic, biodegradable hydrogel can function as a carrier for DBM, and that the volume of bone augmentation achieved by the constructs correlated directly to DBM dose.

Keywords

oligo(poly(ethylene glycol) fumarate); demineralized bone matrix; bone augmentation

1. Introduction

Bone augmentation can be broadly defined as the formation of bone beyond the existing skeletal envelope at an orthotopic skeletal site. Bone augmentation may be attempted in the vertical or lateral direction in a variety of geometries and may be required for functional and/or aesthetic restoration. Inadequate bone volume may result from tooth extraction,

*To whom correspondence should be addressed: Antonios G. Mikos, Ph.D., Rice University, Department of Bioengineering, MS-142, P.O. Box 1892, Houston, TX 77251-1892, Tel: (713) 348-5355, mikos@rice.edu.

disease, trauma, tumor resection, and other causes of deformities. Edentulous patients may require bone augmentation for implant placement, and the disease causing tooth loss may interfere with the effectiveness of bone augmentation procedures [1].

Clinical indications for augmentation surgery include alveolar ridge, sinus, or contour deficits. Alveolar ridge augmentation treats deficits of the 3 classes in the bucco-lingual and/or apico-coronal direction, which may involve shortage of width and/or height [1]. Sinus augmentation treats the atrophic posterior maxilla to enhance bone volume for implant placement [2]. Contour deficits are characterized by insufficient bone volume or projection at a skeletal site, which disrupts the expected facial contours [3]. Generally, autologous bone is the best grafting material; however, synthetic or other natural materials provide an alternative when autologous bone is unavailable, and off-the-shelf options greatly simplify the procedure [4]. To study bone augmentation in a preclinical animal model, it was essential to use an easily accessible region of compact bone with adequate space for surgery and implantation. As such, we designed a rat model with augmentation of the parietal bone in order to meet the above requirements, the parietal bone model having been established in the literature with clear success [5–8].

Oftentimes, interventions of the above sort employ demineralized bone matrix (DBM), the acid-extracted organic matrix of bone. DBM functions as an osteoinductive and osteoconductive biomaterial delivering osteogenic growth factors in a bioresorbable form [9]. Commercial DBM formulations often employ excipients, inactive substances primarily added to enhance the handling properties [3]. Biopolymer excipients lack significant tunability and suffer from irreproducibility compared to synthetic materials [10]. Using an excipient neglects the potential of the carrier phase to augment the osteogenic activity of the DBM. Some researchers have attempted to enhance DBM by adding growth factors including BMP-2 [11], VEGF [12], and TGF-β1 [13]; however, considerable interest and opportunity remains to explore the enhancement of any of these systems with the added flexibility of a synthetic drug delivery system.

Synthetic hydrogels such as oligo(poly(ethylene glycol) fumarate) (OPF) have the potential to enhance the osteogenic effect of DBM as injectable formulations for cell encapsulation and controlled drug release [14]. To that end, we investigated whether OPF, in a simple and unmodified form, could serve as a suitable delivery system for DBM. We hypothesized that, in a rat model of bone augmentation, greater bone volume and height would be achieved by OPF constructs with higher DBM content owing to the greater dose of osteogenic material and to accelerated degradation.

2. Materials and Methods

2.1 Experimental design

The study was split into two parts. The first aimed at designing and testing the fabrication process, elucidating the influence of DBM content and particle size on the physical properties of the constructs, and testing the bioactivity of the DBM. The second part aimed at investigating the constructs in the rat bone augmentation model and evaluating gross

appearance, augmented bone volume, maximum height, and overall tissue appearance by histology. The constructs formulated to complete the study design are listed in Table 1.

2.2 OPF synthesis

OPF was synthesized from poly(ethylene glycol) (PEG) (Sigma Aldrich, St. Louis, MO) with nominal number average molecular weight of 3,350 Daltons (Da) as reported [14]. The resulting OPF had number average molecular weight (M_n) 7500 ± 200 Da and weight average molecular weight (M_w) 36,300 ± 600 Da as determined by gel permeation chromatography using a Waters system with a Styragel HR 4E column and chloroform solvent. The molecular weight was determined using a PEG standard curve.

2.3 DBM harvest and processing

DBM was harvested from the tibiae and femora of 12 week, Fischer 344, male rats based on reported methods [15, 16] under the authorization of the Rice University Institutional Animal Care and Use Committee. Briefly, bilateral tibiae and femora were harvested and soft tissue was removed. The bone ends were removed and bone marrow was flushed with PBS. Bones were crushed to yield bone fragments on the mm size scale. Fragments were placed in 95% ethanol at 4°C for 16 h. The fragments were then moved to ethyl ether at 4°C for 6 h. The bone fragments were filtered and dried. The fragments were further pulverized in a mortar and pestle and sieved to achieve fractions in the range of 50–150 and 150–250 μm. The DBM particle fractions were demineralized in 0.6 M HCl at 4°C for 14 h then filtered and dried. DBM particles were stored at −20°C.

2.4 Composite fabrication

In the present study, our delivery system was produced by mixing OPF hydrogel precursors with DBM particles and cross-linking the OPF creating a hydrogel composite. Composites were fabricated at a size matching the implants for the animal experiment (8 mm diameter x 1 mm height) using an established method [17] as follows. Dry components, OPF, PEG-diacrylate (Glycosan BioSystems, Inc., Alameda, CA), and DBM, were combined and added to PBS. Thermal radical initiators, ammonium persulfate and tetramethylethylenediamine (Sigma Aldrich, St. Louis, MO), were added to initiate crosslinking and the mixture was injected in a Teflon mold and incubated at 37°C for 8 min for crosslinking to proceed. After 8 min, the composite hydrogels were removed from the mold and cultured *in vitro* or implanted in the rat. For the *in vitro* study, constructs were placed in 24 well plates in 1 ml PBS or PBS supplemented with 400 ng/ml collagenase 1A (Sigma Aldrich, St. Louis, MO) (Col PBS) to mimic the level of enzymatic digestion that would occur *in vivo*[18]. Composites were maintained at 37°C on a shaker table at 70 rpm with medium changes after 1 day and continuing twice weekly.

2.5 *In vitro* histology

Histology of *in vitro* samples was performed by embedding composite hydrogels in Histoprep freezing media and making 10 μm frozen sections using a cryotome (Leica 1850CM UV). Sections were stained with Picrosirius Red to reveal the collagen matrix of the DBM particles. Images were taken using a light microscope (Nikon Eclipse E600).

2.6 Physical characterization

The composite hydrogels in the present study were characterized in terms of their degradation, mass swelling, and compressive mechanical properties according to reported methods [19]. Degradation or normalized mass was measured as the fraction of dry mass remaining at day 1 and at 1, 3, and 5 weeks relative to the dry mass at day 0 (n=3 samples). Mass swelling was measured as the ratio of wet weight to dry weight of the samples at each time point at day 1 and at 1, 3, and 5 weeks (n=3). Compressive mechanical properties were measured at 1, 3, and 5 weeks on a Thermomechanical Analyzer (TMA 2940, TA Instruments, New Castle, DE) at a compression rate of 0.1 N/min where the compressive modulus was determined as the initial slope of the stress-strain curve (n=3).

2.7 Osteogenesis assessment

The relative osteogenic activity of DBM was determined using the C2C12 cell line assay (ATCC) [20]. C2C12 cells were expanded in high glucose DMEM medium with 10% fetal bovine serum (BenchMark™ FBS, Gemini Bio-Products, West Sacramento, CA) for several days. C2C12 cells were lifted with 0.25% trypsin and seeded at 50,000 cells per well in a 24 well culture plate and allowed to attach overnight (n=5). Medium was replaced with high glucose DMEM with 1% FBS for the control or supplemented with 4 mg/ml DBM (based on previous experiments that investigated this concentration[20]) with particle size of 50–150 μm for the test. Alkaline phosphatase (ALP) activity (nmoles p-Nitrophenol/h) was determined and normalized to DNA (μg).

2.8 Animal surgeries

Animal surgeries were performed under the authorization and guidance of the Rice University Institutional Animal Care and Use Committee and complete NIH requirements were followed (NIH Publication #85-23 Rev. 1985). Surgery was performed on 24 animals (12 week, Fischer 344, male rats) divided into 3 groups (n=8 per group). The groups consisted of an empty Teflon ring and two composites with a DBM:OPF ratio of 1:1 or 3:1. The surgical procedure and surgical setup were adapted from previous studies [5, 17]. General anesthesia and postoperative care were performed in a typical manner for surgeries of this type [21]. The surgical procedure involved making a sagittal incision through the skin over the parietal bone from approximately 2–3 mm anterior the coronal suture to 2–3 mm posterior the lambdoid suture. A matching incision was made in the periosteum and the tissue was carefully resected. A groove 0.3 mm in depth was drilled using an 8 mm trephine bur in the parietal bone centered over the sagittal suture and just anterior to the lambdoid suture. A Teflon ring of 1.3 mm height and 8 mm inner diameter was fit inside the groove. After placing the implant inside the ring, the periosteum and skin were sutured in two layers using running 5-0 and 4-0 Vicryl resorbable sutures, respectively. Animals were administered systemic analgesia for a period of 36 h following surgery.

2.9 Tissue harvest

After 12 weeks implantation, animals were euthanized under isoflurane anesthesia by CO_2 asphyxiation. Skulls were harvested using a cutting bur on a dental drill unit after blunt

dissection of the overlying soft tissue leaving the periosteum intact. Specimens were fixed in 10% neutral buffered formation for 72 h and dehydrated in 70% ethanol.

2.10 Microcomputed tomography analysis

Microcomputed tomography (μCT) was performed on samples in 70% ethanol as described previously [17]. Scans were performed at 40 kV and 250 mA on a SkyScan 1172 high-resolution micro-CT (Bruker, Belgium). Bone volume in the region of interest was determined with a thresholding range of 70–250. The region of interest was 8 mm diameter x 1 mm height to match the implant dimensions. The position of the region of interest was determined according to the uniform height of the Teflon ring and thickness of the parietal bone between animals to ensure accurate positioning.

2.11 Histological analysis

Specimens were dehydrated in a series of ethanol and decalcified in 60 ml Formical 2000 (Decal Chemical Corp. Tallman, NY) with weekly refreshment for 3 weeks. Specimens were soaked for 1 h in 15% sucrose, soaked overnight in 30% sucrose, and then embedded in Histoprep freezing media and frozen at −60°C. Specimens were sectioned to 6 μm thickness using a cryotome (Leica 1850CM UV). Sections were stained with hematoxylin and eosin (H&E) and imaged on a Zeiss Axioimager Z2 light microscope.

2.12 Statistics

Data are reported as mean ± standard deviation. Statistical analysis was performed using one-way ANOVA and Tukey's HSD post-hoc test with a priori significance set to $\alpha=0.05$.

3. Results

3.1 *In vitro* histology

Histological sections were made using 3:1 constructs with 50–150 μm DBM to demonstrate the qualitative morphology of the DBM particles as well as their distribution in the composites. A representative image is shown in Figure 1 although histology was performed to confirm the particle morphology and homogeneous distribution in the other groups. Morphology and distribution of the particles in 1:1 constructs is demonstrated in the *in vivo* histology section. According to Figure 1 the size range is confirmed according to the expected result of the sieving process, and particles appear as irregular polygons owing to the nature of their processing.

3.2 Degradation

Degradation is reported in terms of normalized mass relative to the dry mass of each group at day 0 as shown in Figure 2. Within each group the degradation increased as culture progressed. An increase in DBM content correlated to faster degradation of hydrogels often resulting in total degradation by 5 weeks. For DBM particle size of 50–150 μm, 3:1 constructs degraded in as little as 1 week whereas 1:1 constructs degraded within 5 weeks. 1:3 constructs degraded relatively little, still retaining half their original mass at 5 weeks. For particle size of 150–250 μm, 3:1 constructs degraded in only 1 day, while 1:1 and 1:3 constructs did not degrade within 5 weeks. Culture in collagenase PBS did accelerate the

degradation of the 1:1 constructs by 5 weeks, but no other effect of collagenase was observed. Comparing between particle sizes, 3:1 constructs with 150–250 μm DBM degraded most quickly whereas degradation was accelerated in 1:1 constructs with 50–150 μm DBM.

3.3 Mass swelling

Mass swelling is reported in terms of the wet weight to dry weight mass ratio at each time point as shown in Figure 3. The data are not reported for any constructs that degraded prior to the time point for swelling measurement. Within each group the swelling increased as culture progressed. Of significance, 3:1 constructs with 50–150 μm DBM had a lower mass swelling than other DBM contents, and for 150–250 μm DBM in collagenase, 1:1 constructs had greater swelling than 1:3 constructs at 3 weeks.

3.4 Mechanical testing

A general measure of the mechanical properties of the constructs was determined by measuring the compressive modulus of each construct. The compressive moduli are shown in Figure 4. No data are reported for 3:1 constructs because they had degraded prior to the earliest time point of study, and any other constructs that degraded prior to a predefined time point could not be included in the analysis. Within each group the compressive modulus decreased as culture progressed.

After culture time, DBM content exhibited the most significant effect on compressive modulus with more DBM incorporation correlating to lesser mechanical properties. Specifically, 1:3 constructs had greater moduli for 50–150 μm DBM at 1 week for both media types and at 3 weeks for PBS and for 150–250 μm DBM at 1 week for collagenase and 3 weeks for PBS. 50–150 μm DBM lowered the compressive moduli of 1:3 constructs in PBS at 1 and 3 weeks and of 1:1 constructs in PBS at 1 week. Culture in collagenase regularly reduced the compressive moduli of 1:3 constructs at 3 weeks for both particle sizes. Collagenase also reduced the moduli of 1:3 constructs with 150–250 μm particles at 5 weeks and 1:1 constructs with 150–250 μm particles at 1 week.

3.5 Osteogenesis assessment

The relative baseline level of osteogenic activity of the DBM particles was determined by a standard C2C12 cell culture assay. The results are shown graphically in Figure 5. After a 2-day culture, the normalized ALP expression in the control group was unchanged whereas supplementation with 4 mg/ml DBM particles (50–150 μm) increased the level of ALP expression 4-fold ($p<0.05$).

3.6 *Ex vivo* gross appearance

At the time of specimen harvest after soft tissue dissection, gross images were taken to record qualitatively the nature of the tissue in and around the Teflon ring and implant. Representative images from each group are displayed in Figure 6. The Teflon ring is visible through the periosteum in the transverse views. In Figure 6, the empty group (A) showed a lack of significant tissue volume within the implant site, while the 1:1 (B) and 3:1 (C) constructs demonstrated tissue and/or material filling up to the maximum height of the ring,

which is visible in the images. The 1:1 group appeared to contain a significant amount of OPF hydrogel as evidenced by the perimeter of the hydrogel disk indicated by the arrow in (B).

3.7 Microcomputed tomography analysis

The volume of augmented bone was determined from μCT images, and the results are shown in Figure 7B. The augmented volume refers to the absolute volume of bone that formed beyond the existing skeletal envelope during the 12-week implant duration as defined above. The empty, 1:1, and 3:1 groups achieved approximately 2, 3, and 10 mm^3 of bone formation, respectively. Accordingly, the 3:1 constructs achieved a 5-fold increase in augmentation compared to the empty control group and a 3-fold increase compared to the 1:1 constructs ($p<0.05$).

The maximum height of augmented bone beyond the existing skeletal envelope was determined from the μCT images, and the results are shown in Figure 7C. Regions of bone augmentation facilitated by conduction along the Teflon ring were excluded from the measurement to negate the influence of the augmentation model in this outcome. The maximum height refers to the maximum height of bone augmentation achieved superior to the native bone surface at 12 weeks within the region of interest defined earlier, which was implemented in the augmented bone volume measurement. The empty, 1:1, and 3:1 groups achieved approximately 0.19, 0.64, and 0.69 mm of maximum bone height, respectively. Accordingly, the 3:1 and 1:1 constructs achieved at least a 3-fold increase in maximum bone height compared to the empty control group ($p<0.05$).

3.8 *In vivo* histology

H&E staining was performed and representative sections are shown in Figure 8. In all groups, bone formed predominantly from the parietal bone surface with location varying by sample from exclusively around the sagittal suture to only on the periphery and anything in between. Compact bone was formed in each group. Bone tended to conduct along the inside edges of the Teflon ring in all groups. Greater volume of bone was consistently formed in the 3:1 group. OPF was observed within in the 3:1 and 1:1 groups at 12 weeks. Greatest bone volume directly correlated to greater soft tissue volume in the 3:1 implants.

3:1 constructs generated a large volume of both hard and soft tissue within the implant site. DBM particles undergoing remodeling were observed in the augmented bone region with unremodeled particles present in regions with only soft tissue present or where OPF was still present at 12 weeks. DBM particles were homogeneously distributed at relatively high density. Constructs appear to have retained much less of their original height in the center part of the implant near the sagittal suture compared to the lateral portions.

1:1 constructs generated relatively little tissue within the implant site. DBM particles were predominately unremodeled and remained encapsulated in OPF at 12 weeks. Particles were homogenously distributed with relatively low density compared to 3:1 constructs. Constructs appeared to maintain their original shape to a larger extent than 3:1 constructs.

The empty group generated negligible tissue within the boundaries of the Teflon ring with the periosteum regaining its placement immediately superior to the native bone. Bone augmentation was localized to the periphery of the implant site with maximum bone height formed adjacent to the Teflon ring.

4. Discussion

The present work investigated a new synthetic hydrogel system for the delivery of DBM. Constructs were fabricated with DBM homogenously dispersed within the biodegradable hydrogel, OPF. We first investigated the fabrication of constructs, the effect of DBM content and particle size on construct physical properties, and the osteogenic activity of the DBM. In the second part of the study, we investigated the ability of the hydrogel carrier to deliver DBM for bone augmentation and answered the question of whether constructs with higher DBM content would result in greater bone augmentation in volume and height by μCT and histological appearance.

On construct fabrication, Picrosirius Red staining was implemented in the histological analysis of *in vitro* samples to visualize DBM particles by their high collagen content. The particles were homogeneously distributed throughout the hydrogel, which is important to the consistency of the approach, and no problems were observed during the fabrication such as agglomeration or precipitation of the particles. Further, the individual particle size appears in the appropriate range from the sieving process, and the morphology is consistent with typical DBM preparation [22]. Finally, construct fabrication proved to be a reproducible process helping to ensure experimental accuracy.

The results from degradation, mass swelling, and mechanical testing together describe the physical characteristics of the constructs and their dependence on fabrication parameters including DBM content, DBM particle size, and media type. Because of the inherent degradative property of OPF [23], and the interdependence of the various physical measures [19], all constructs exhibited degradation, increased swelling, and decreased mechanical properties over the course of study. With higher DBM content, constructs had accelerated degradation, increased swelling, and lower mechanical properties, outcomes consistent with the effect of increasing the content of a degradable gelatin microparticle porogen in these hydrogels [19]. Thus the DBM content provides a means of tuning the physical properties of these constructs as well as delivering the bioactive material at various dosages.

Focused upon the aim of investigating the effect of DBM content *in vivo*, the physical characterization was performed to evaluate and understand the suitability of different particle sizes for the physical performance of the constructs. DBM particle size had some effect on the physical properties of the constructs with the exception of swelling. 50–150 μm DBM tended to lower the mechanical properties of 1:3 and 1:1 constructs in PBS at early time points and to result in faster degradation in 1:1 constructs by 5 weeks. The 50–150 μm particles have greater surface area to volume ratio, which increases the interfacial area between the hydrogel matrix and DBM particles. This change combined with the difference in individual volume swelling of the two materials likely had a disruptive effect on the OPF matrix that scaled with the size of the interface resulting in the observed effect on physical

properties [19]. Collagenase culture was implemented along with PBS culture to more fully understand the potential effects of DBM content and particle size in an environment more similar to that of conditions experienced *in vivo* [24]. The effect of collagenase culture was of varying importance to the different physical measures in the present study. With regard to degradation and mass swelling the effect of collagenase was limited; however collagenase culture regularly lowered the mechanical properties of the constructs by 3 weeks. To explain this effect, individual DBM particles composed of collagen undergo bulk degradation in the presence of the enzyme. At an intermediate state, reduced crosslinking density allows greater volume swelling of the DBM, which mechanically disrupts the surrounding OPF matrix [24]. This effect reduces the mechanical properties of the construct without greatly influencing degradation or mass swelling thus showing the potential effect of *in vivo* culture conditions on construct mechanical properties.

In summary, we established a proof of concept for using OPF as a delivery system for DBM, and DBM content and particle size had important effects on the various physical properties investigated. The 50–150 μm particle size range presented the most favorable option for further *in vitro* and *in vivo* testing based on accelerated degradation of the 1:1 constructs, better handling properties of the 3:1 constructs, and increased surface area for tissue contact and remodeling. Furthermore, 1:1 and 3:1 constructs were investigated *in vivo* due to their accelerated degradation.

An *in vitro* assay was utilized in this work to confirm the osteogenic activity of the rat-derived DBM. The induction of C2C12 cells to upregulate their production of ALP is an established method of determining the relative osteogenic potential of various materials [20, 25, 26], and the method has been validated against an *in vivo* osteoinductivity model [20]. The DBM particles evaluated in the present work maintained high levels of osteogenic bioactivity as evidenced by the upregulation of ALP 4-fold compared to the control culture. Considering the use of established methods for its preparation and its osteogenic activity, the DBM utilized in the present work was expected to display bioactivity *in vivo*.

The present work implemented a new surgical setup for bone augmentation in the rat shown schematically in Figure 7A. Our model was designed in large part based on lessons learned from two previous models in the rat. In the first, investigators implanted two anterior/posterior implants (6 mm diameter, 2 mm height) per rat within groove-immobilized Teflon rings, and the authors used the model for the study of porous CPC [5]. In the second study, our laboratory implanted two left/right implants (6 mm diameter, 2 mm height) per rat within screw-immobilized polypropylene cassettes [17]. Though less influential to our design, others have used subperiosteal pockets [7, 27–30], non-immobilized rings [6, 31], and groove [8, 32] or screw immobilization [33–35]. Our new model has the advantage of matching the dimensions of the rat critical-sized calvarial defect (8 mm diameter) [36] allowing scaffolds to be tested directly for bone augmentation without repeating *in vitro* characterization. Our model also incorporates advantages of previous models such as rigid immobilization to prevent micromotion and use of the Teflon ring to prevent soft tissue compression of the implant.

Recognizing the potential hindrance to bone augmentation of having degradation proceed more slowly than tissue ingrowth in hydrogel constructs [17], designing constructs that completely degraded *in vitro* on an abbreviated timescale would be promising to the application of these constructs *in vivo*. Even *in vitro* degradation periods as brief as 1 week like we observed in some groups would be expected to scale to several weeks *in vivo* providing adequate support for bone induction based on the correlation of *in vitro* and *in vivo* degradation rates observed previously in composite hydrogels [37]. This outcome was observed whereby 3:1 constructs degraded almost entirely within 12 weeks *in vivo* evidenced by histology sectioning. Thus, the more rapid degradation proved to suit the augmentation strategy by providing more void space for bone augmentation compared to the more slowly degrading 1:1 constructs, which remained largely intact at study completion. This result gleaned from histology aligned with observations of the gross appearance of 1:1 constructs as shown in Figure 6.

As to the animal model implemented in the present study, the *ex vivo* images show excellent gross healing of the periosteum, complete degradation of the subcutaneous sutures, reproducible and immobile placement of the Teflon ring, and lack of noticeable deformation of the ring with time. The most definitive single measure to the outcome of a scaffold-based approach to bone augmentation is the total volume of augmented bone in the implant site. Traditionally, augmented bone volume has been determined by either histomorphometry or μCT. Histomorphometry has the inherent drawback of providing a segmented view of the region of interest based on the spacing of sections on which the calculation is performed followed by averaging and scaling the result [31, 32]. μCT on the other hand, provides a complete view of the region of interest [8, 17, 38]. As such, we employed μCT imaging in the present investigation to quantify new bone formation and histology for qualitative information about the new tissue formation. The DBM content of the constructs had a significant impact on the volume of bone augmented. 3:1 constructs produced more than 3-fold greater bone volume compared to the 1:1 constructs and 5-fold greater bone compared to the empty controls. Coincidentally, 3:1 constructs contained a 3-fold greater concentration of DBM compared to 1:1 constructs, and ectopic bone volume has been shown to vary linearly with DBM dose [39]. While the incorporation of DBM likely acts dose-dependently based on its osteogenic bioactivity [20], the changes in construct physical properties have potential to significantly affect the outcome by way of accelerated degradation of the OPF hydrogels. In previous studies, when OPF hydrogels showed delayed degradation *in vivo*, tissue ingrowth was hindered [17, 40]. According to our histology, the 1:1 constructs retained a high proportion of OPF within the implant site at 12 weeks, which likely inhibited tissue ingrowth and prevented significant augmentation from occurring. The 3:1 constructs, on the other hand, are mostly void of OPF at 12 weeks, indicating accelerated degradation, which would have enabled tissue ingrowth to occur more freely and result in greater augmentation.

While the results of total augmented bone volume varied due to DBM content, the maximum height of augmented bone was similar between 3:1 and 1:1 constructs, both exceeding the empty control by at least 3-fold. From μCT, 3:1 constructs often displayed robust augmentation with interconnected bone spanning from the native surface to the maximum

height. However, 1:1 constructs often resulted in a somewhat more disconnected bone structure whereby the maximum height was achieved by a rogue bone nucleation site. 1:1 constructs then show potential to perform well in terms of augmented bone volume but may require a longer time to allow greater OPF degradation in order to match the performance of the 3:1 constructs.

Finally, the histology staining was able to extend, explain, and reinforce the many notable outcomes already described. Compression of augmentation implants due to tension in the overlying soft tissue has been shown to reduce total bone augmentation [6]. The 3:1 implants showed height reduction in their center by histology; however, the effect did not reduce the volume of bone augmented in that region compared to the periphery showing that the model used was capable of projecting the potential of the treatment in the absence of compressive forces.

To our knowledge, the present study represents the first application of a synthetic hydrogel for the delivery of DBM for bone augmentation. Besides functioning as an excellent inert carrier, OPF can be utilized for encapsulation of mesenchymal stem cells [41], growth factor [42] or gene delivery [43], and incorporation of cell binding moieties [44], or other osteoconductive domains [45, 46]. Thus, the OPF hydrogel presents a platform technology for future development of the carrier phase to augment the osteogenic bioactivity of DBM.

5. Conclusion

The present work evaluated the bone augmenting effect of DBM delivered via OPF synthetic hydrogels. Rat-derived DBM demonstrated osteogenic activity and constructs could be fabricated with homogeneous particle dispersion. The physical properties of the constructs were evaluated, and we observed degradation, increased mass swelling, and decreased mechanical properties with culture time. Higher content of DBM accelerated those changes, and variation due to particle size was dependent on the content as well. The effect of DBM content was investigated in a vertical augmentation model in the rat, and we observed a dose dependent effect of DBM on the volume of bone augmentation but not on maximum height. The results were confirmed and further explained by histological staining. Altogether an innovative DBM delivery system is provided.

Acknowledgments

The research described in this manuscript was supported by grants from the Armed Forces Institute of Regenerative Medicine (W81XWH-08-2-0032) and the National Institutes of Health (R01 AR048756). L.A.K. and E.J.L. acknowledge support from a National Science Foundation Graduate Research Fellowship.

References

1. McAllister BS, Haghighat K. Bone augmentation techniques. J Periodontol. 2007; 78:377–396. [PubMed: 17335361]
2. Browaeys H, Bouvry P, De Bruyn H. A literature review on biomaterials in sinus augmentation procedures. Clin Implant Dent Relat Res. 2007; 9:166–177. [PubMed: 17716261]
3. Gruskin E, Doll BA, Futrell FW, Schmitz JP, Hollinger JO. Demineralized bone matrix in bone repair: History and use. Adv Drug Deliv Rev. 2012; 64:1063–1077. [PubMed: 22728914]

4. Sbordone C, Toti P, Guidetti F, Califano L, Pannone G, Sbordone L. Volumetric changes after sinus augmentation using blocks of autogenous iliac bone or freeze-dried allogeneic bone. A non-randomized study. J Craniomaxillofac Surg. 2014; 42:113–118. [PubMed: 23726762]
5. Klijn RJ, et al. Three different strategies to obtain porous calcium phosphate cements: Comparison of performance in a rat skull bone augmentation model. Tissue Eng Part A. 2012; 18:1171–1182. [PubMed: 22292519]
6. Matsui A, et al. Mechanical stress-related calvaria bone augmentation by onlayed octacalcium phosphate-collagen implant. Tissue Eng Part A. 2010; 16:139–151. [PubMed: 19642866]
7. Martinez-Sanz E, Ossipov DA, Hilborn J, Larsson S, Jonsson KB, Varghese OP. Bone reservoir: Injectable hyaluronic acid hydrogel for minimal invasive bone augmentation. J Control Release. 2011; 152:232–240. [PubMed: 21315118]
8. Kochi G, Sato S, Ebihara H, Hirano J, Arai Y, Ito K. A comparative study of microfocus ct and histomorphometry in the evaluation of bone augmentation in rat calvarium. J Oral Sci. 2010; 52:203–211. [PubMed: 20587943]
9. Holt DJ, Grainger DW. Demineralized bone matrix as a vehicle for delivering endogenous and exogenous therapeutics in bone repair. Adv Drug Deliv Rev. 2012; 64:1123–1128. [PubMed: 22521662]
10. Vo TN, Kasper FK, Mikos AG. Strategies for controlled delivery of growth factors and cells for bone regeneration. Adv Drug Deliv Rev. 2012; 64:1292–1309. [PubMed: 22342771]
11. Chen B, et al. Homogeneous osteogenesis and bone regeneration by demineralized bone matrix loading with collagen-targeting bone morphogenetic protein-2. Biomaterials. 2007; 28:1027–1035. [PubMed: 17095085]
12. Emad B, Sherif E, Basma GM, Wong RW, Bendeus M, Rabie AB. Vascular endothelial growth factor augments the healing of demineralized bone matrix grafts. Int J Surg. 2006; 4:160–166. [PubMed: 17462340]
13. Gombotz WR, Pankey SC, Bouchard LS, Ranchalis J, Puolakkainen P. Controlled release of tgf-beta 1 from a biodegradable matrix for bone regeneration. J Biomater Sci Polym Ed. 1993; 5:49–63. [PubMed: 8297831]
14. Kinard LA, Kasper FK, Mikos AG. Synthesis of oligo(poly(ethylene glycol) fumarate). Nat Protoc. 2012; 7:1219–1227. [PubMed: 22653160]
15. Kurkalli BG, Gurevitch O, Sosnik A, Cohn D, Slavin S. Repair of bone defect using bone marrow cells and demineralized bone matrix supplemented with polymeric materials. Curr Stem Cell Res Ther. 2010; 5:49–56. [PubMed: 19807659]
16. Carpenter EM, Gendler E, Malinin TI, Temple HT. Effect of hydrogen peroxide on osteoinduction by demineralized bone. Am J Orthop. 2006; 35:562–567. [PubMed: 17243405]
17. Kinard LA, et al. Tissue response to composite hydrogels for vertical bone augmentation in the rat. J Biomed Mater Res A. 2013
18. Kinard LA, Chu CY, Tabata Y, Kasper FK, Mikos AG. Bone morphogenetic protein-2 release from composite hydrogels of oligo(poly(ethylene glycol) fumarate) and gelatin. Pharm Res. 2013
19. Kinard LA, Chu CY, Tabata Y, Kasper FK, Mikos AG. Bone morphogenetic protein-2 release from composite hydrogels of oligo(poly(ethylene glycol) fumarate) and gelatin. Pharm Res. 2013; 30:2332–2343. [PubMed: 23686376]
20. Han B, Tang B, Nimni ME. Quantitative and sensitive in vitro assay for osteoinductive activity of demineralized bone matrix. J Orthop Res. 2003; 21:648–654. [PubMed: 12798064]
21. Patel ZS, Young S, Tabata Y, Jansen JA, Wong ME, Mikos AG. Dual delivery of an angiogenic and an osteogenic growth factor for bone regeneration in a critical size defect model. Bone. 2008; 43:931–940. [PubMed: 18675385]
22. Dumas JE, Zienkiewicz K, Tanner SA, Prieto EM, Bhattacharyya S, Guelcher SA. Synthesis and characterization of an injectable allograft bone/polymer composite bone void filler with tunable mechanical properties. Tissue Eng Part A. 2010; 16:2505–2518. [PubMed: 20218874]
23. Temenoff JS, Park H, Jabbari E, Conway DE, Sheffield TL, Ambrose CG, Mikos AG. Thermally cross-linked oligo(poly(ethylene glycol) fumarate) hydrogels support osteogenic differentiation of encapsulated marrow stromal cells in vitro. Biomacromolecules. 2004; 5:5–10. [PubMed: 14715001]

24. Holland TA, Tessmar JKV, Tabata Y, Mikos AG. Transforming growth factor-beta 1 release from oligo(poly(ethylene glycol) fumarate) hydrogels in conditions that model the cartilage wound healing environment. J Controlled Release. 2004; 94:101–114.
25. Tian M, Yang Z, Kuwahara K, Nimni ME, Wan C, Han B. Delivery of demineralized bone matrix powder using a thermogelling chitosan carrier. Acta Biomater. 2012; 8:753–762. [PubMed: 22079781]
26. Jiao X, Billings PC, O'Connell MP, Kaplan FS, Shore EM, Glaser DL. Heparan sulfate proteoglycans (hspgs) modulate bmp2 osteogenic bioactivity in c2c12 cells. J Biol Chem. 2007; 282:1080–1086. [PubMed: 17020882]
27. Fujita R, Yokoyama A, Kawasaki T, Kohgo T. Bone augmentation osteogenesis using hydroacyapatite and beta-tricalcium phosphate blocks. J Oral Maxillofac Surg. 2003; 61:1045–1053. [PubMed: 12966480]
28. Kuniyasu H, et al. Bone augmentation using a gdf-5-collagen composite. J Bone Miner Res. 1999; 14:S432–S432.
29. Kuniyasu H, Hirose Y, Ochi M, Yajima A, Sakaguchi K, Murata M, Pohl F. Bone augmentation using rhgdf-5-collagen composite. Clin Oral Implants Res. 2003; 14:490–499. [PubMed: 12869012]
30. Murata M, Maki F, Sato D, Shibata T, Arisue M. Bone augmentation by onlay implant using recombinant human bmp-2 and collagen on adult rat skull without periosteum. Clin Oral Implants Res. 2000; 11:289–295. [PubMed: 11168221]
31. Nakajima D, Kamakura S, Nakamura M, Suzuki O, Echigo S, Sasano Y. Analysis of appositional bone formation using a novel rat experimental model. Oral Dis. 2008; 14:308–313. [PubMed: 18410575]
32. Oginuma T, Sato S, Udagawa A, Saito Y, Arai Y, Ito K. Autogenous bone with or without hydroxyapatite bone substitute augmentation in rat calvarium within a plastic cap. Oral Surg Oral Med Oral Pathol Oral Radiol. 2012; 114:S107–113. [PubMed: 23063386]
33. von See C, Gellrich NC, Jachmann U, Laschke MW, Bormann KH, Rucker M. Bone augmentation after soft-tissue expansion using hydrogel expanders: Effects on microcirculation and osseointegration. Clin Oral Implants Res. 2010; 21:842–847. [PubMed: 20345382]
34. Slotte C, Lundgren D. Augmentation of calvarial tissue using nonpermeable silicone domes and bovine bone mineral - an experimental study in the rat. Clin Oral Implants Res. 1999; 10:468–476. [PubMed: 10740456]
35. Lundgren A, Lundgren D, Taylor A. Influence of barrier occlusiveness on guided bone augmentation. An experimental study in the rat. Clin Oral Implants Res. 1998; 9:251–260. [PubMed: 9760900]
36. Spicer PP, Kretlow JD, Young S, Jansen JA, Kasper FK, Mikos AG. Evaluation of bone regeneration using the rat critical size calvarial defect. Nat Protoc. 2012; 7:1918–1929. [PubMed: 23018195]
37. Kim K, et al. Osteochondral tissue regeneration using a bilayered composite hydrogel with modulating dual growth factor release kinetics in a rabbit model. J Control Release. 2013; 168:166–178. [PubMed: 23541928]
38. Saito Y, Sato S, Oginuma T, Saito Y, Arai Y, Ito K. Effects of nicotine on guided bone augmentation in rat calvarium. Clin Oral Implants Res. 2013; 24:531–535. [PubMed: 22276738]
39. Atti E, Abjornson C, Diegmann M, Zhang K, Cammisa FP, Myers ER. High resolution x-ray computed tomography as a technique to study osteoinductivity of demineralized bone matrix. Spine J. 2003; 3:120. 109.
40. Kasper FK, Young S, Tanahashi K, Barry MA, Tabata Y, Jansen JA, Mikos AG. Evaluation of bone regeneration by DNA release from composites of oligo(poly(ethylene glycol) fumarate) and cationized gelatin microspheres in a critical-sized calvarial defect. J Biomed Mater Res A. 2006; 78:335–342. [PubMed: 16639744]
41. Temenoff JS, Park H, Jabbari E, Sheffield TL, LeBaron RG, Ambrose CG, Mikos AG. In vitro osteogenic differentiation of marrow stromal cells encapsulated in biodegradable hydrogels. Journal of Biomedical Materials Research Part A. 2004; 70A:235–244. [PubMed: 15227668]

42. Guo X, et al. Effects of tgf-beta 3 and preculture period of osteogenic cells on the chondrogenic differentiation of rabbit marrow mesenchymal stem cells encapsulated in a bilayered hydrogel composite. Acta Biomater. 2010; 6:2920–2931. [PubMed: 20197126]

43. Kasper FK, Jerkins E, Tanahashi K, Barry MA, Tabata Y, Mikos AG. Characterization of DNA release from composites of oligo(poly(ethylene glycol) fumarate) and cationized gelatin microspheres in vitro. Journal of Biomedical Materials Research Part A. 2006; 78A:823–835. [PubMed: 16741980]

44. Shin H, Temenoff JS, Bowden GC, Zygourakis K, Farach-Carson MC, Yaszemski MJ, Mikos AG. Osteogenic differentiation of rat bone marrow stromal cells cultured on arg-gly-asp modified hydrogels without dexamethasone and beta-glycerol phosphate. Biomaterials. 2005; 26:3645–3654. [PubMed: 15621255]

45. Bongio M, et al. Biomimetic modification of synthetic hydrogels by incorporation of adhesive peptides and calcium phosphate nanoparticles: In vitro evaluation of cell behavior. Eur Cell Mater. 2011; 22:359–376. [PubMed: 22179935]

46. Leeuwenburgh SC, Jansen JA, Mikos AG. Functionalization of oligo(poly(ethylene glycol)fumarate) hydrogels with finely dispersed calcium phosphate nanocrystals for bone-substituting purposes. J Biomater Sci Polym Ed. 2007; 18:1547–1564. [PubMed: 17988519]

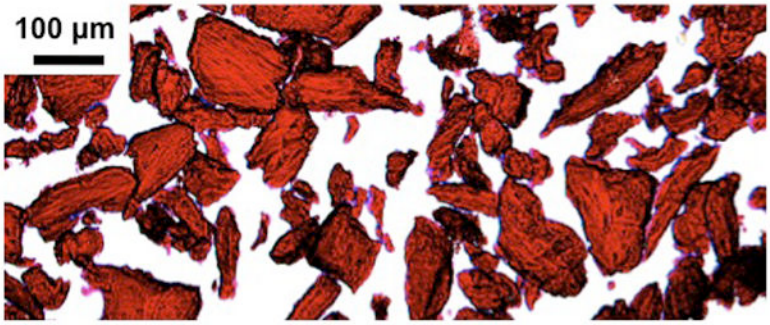

Figure 1.
Picrosirius Red stained 10 μm thin section of a representative 50–150 μm, 3:1 DBM:OPF construct showing red staining for collagen (original magnification 10x).

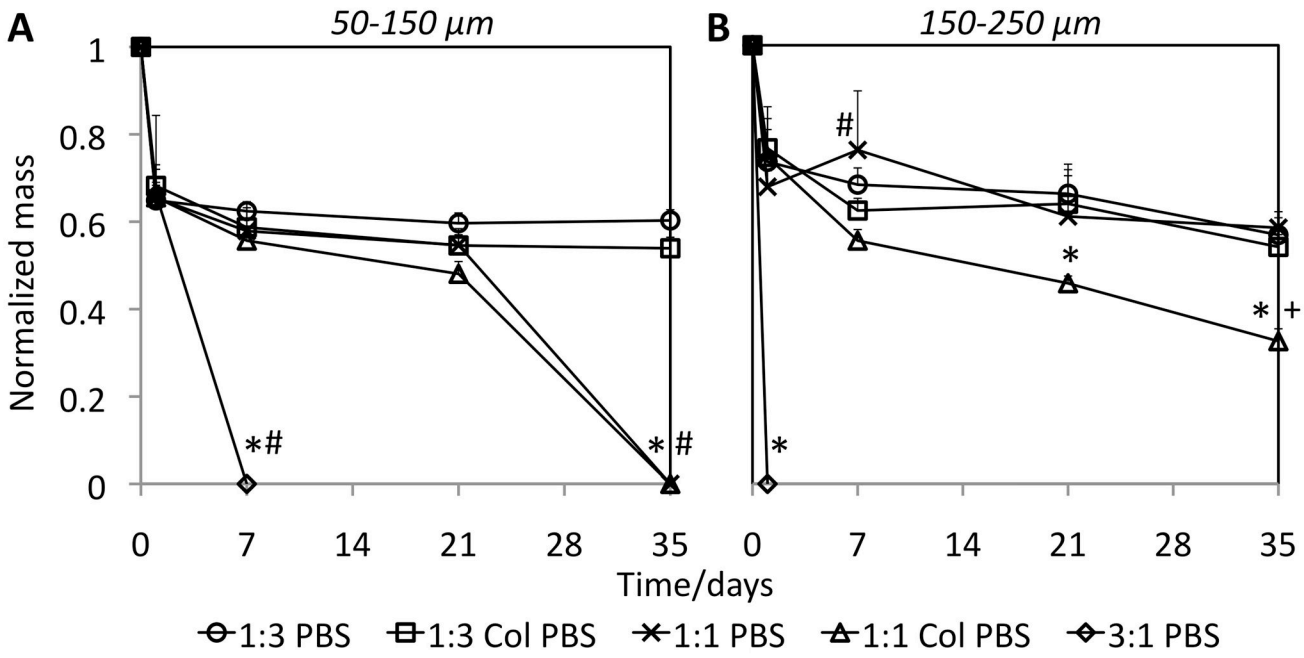

Figure 2.

Degradation of 1:3, 1:1, and 3:1 DBM:OPF constructs in PBS and Col PBS (400 ng/ml collagenase 1A) with 50–150 μm DBM particle size in (A) and 150–250 μm in (B). Error bars indicate + 1 standard deviation from the mean (n=3). Significant differences at each time point are indicated by * for DBM content, # for DBM particle size, and + for collagenase culture ($p<0.05$).

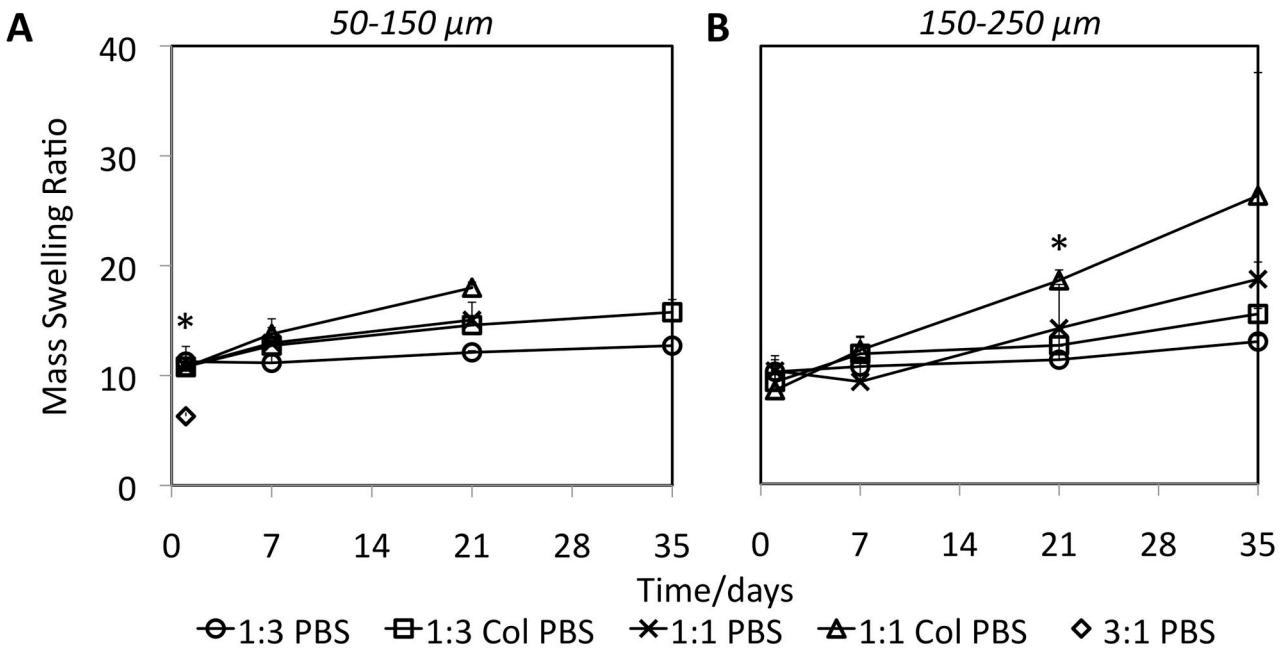

Figure 3.

Mass swelling of 1:3, 1:1, and 3:1 DBM:OPF constructs in PBS and Col PBS (400 ng/ml collagenase 1A) with 50–150 μm DBM particle size in (A) and 150–250 μm in (B). Error bars indicate + 1 standard deviation from the mean (n=3). Significant differences at each time point are indicated by * for DBM content ($p<0.05$).

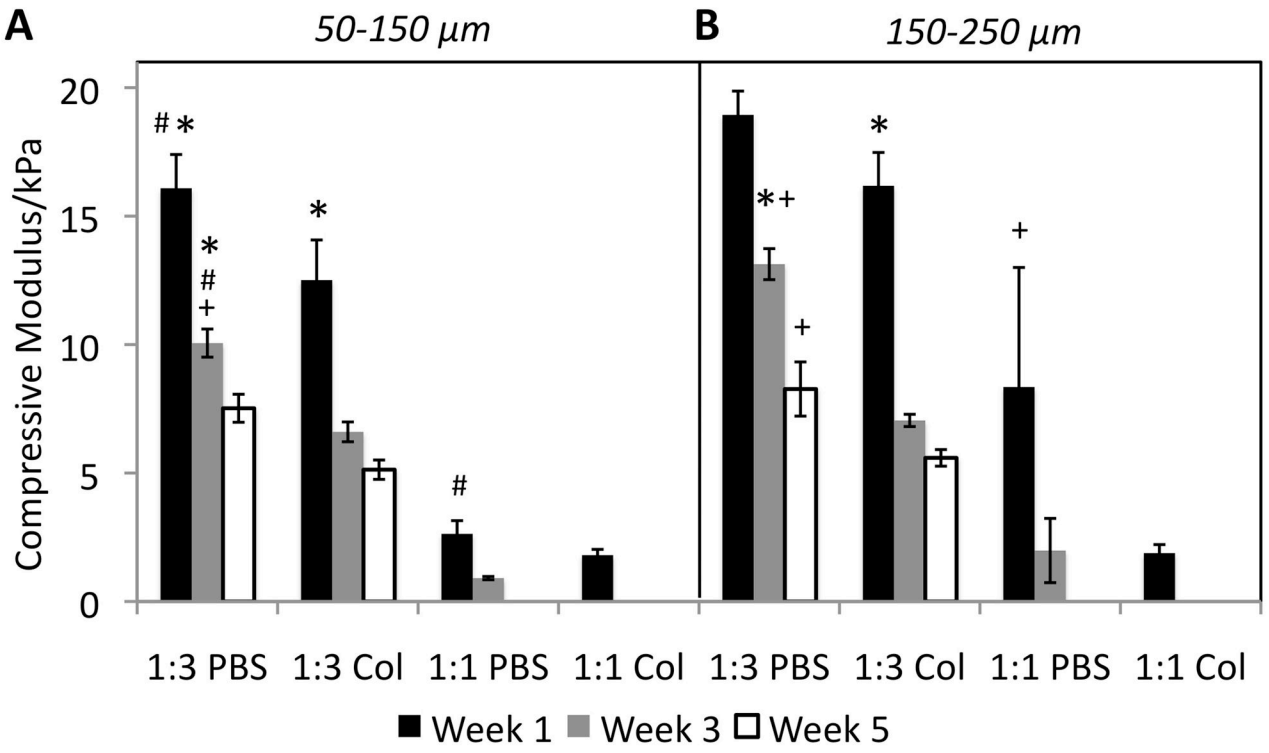

Figure 4.

Compressive moduli of 1:3 and 1:1 DBM:OPF constructs in PBS and Col PBS (400 ng/ml collagenase 1A) with 50–150 µm DBM particle size in (A) and 150–250 µm in (B). Error bars indicate ± 1 standard deviation from the mean (n=3). Significant differences at each time point are indicated by * for DBM content, # for DBM particle size, and + for collagenase culture ($p<0.05$).

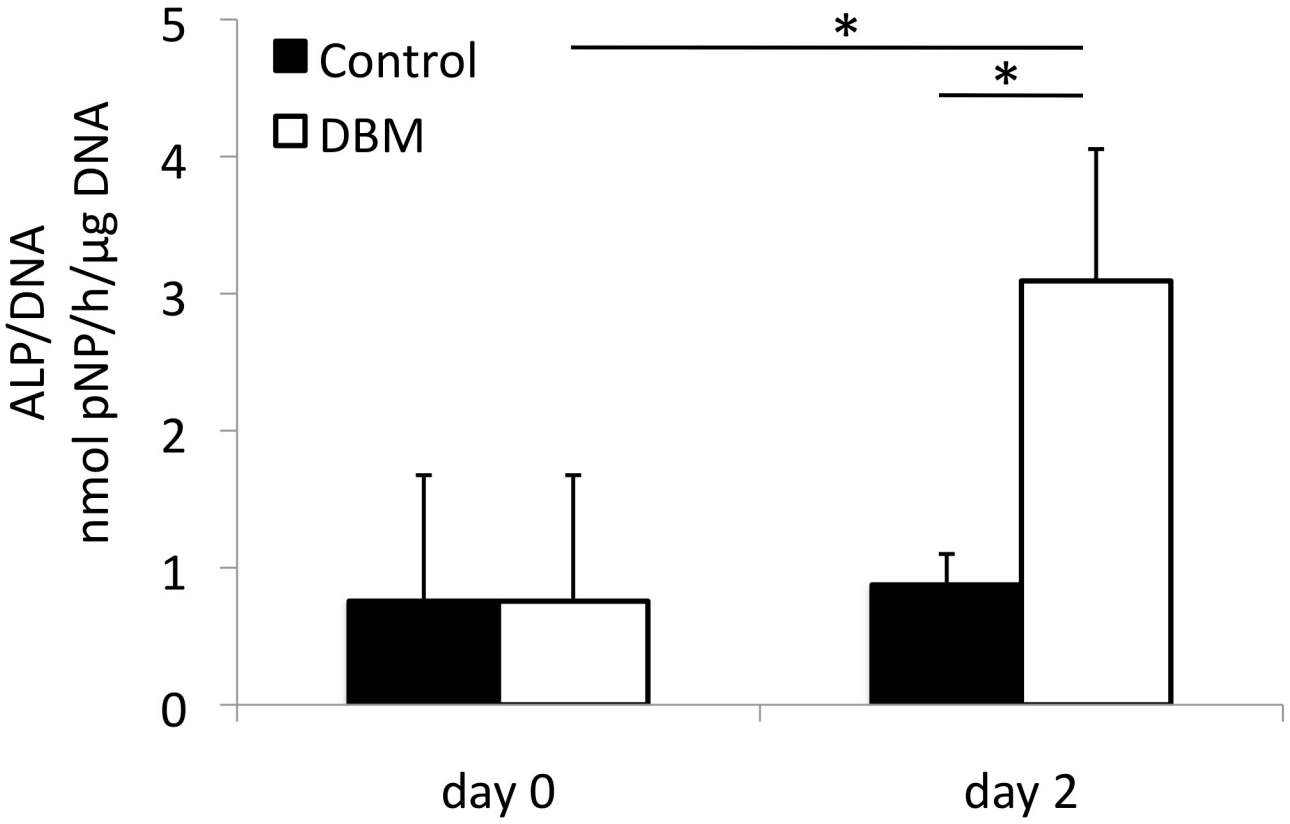

Figure 5.

Normalized ALP levels for C2C12 cells cultured in general media (control) or general media supplemented with 4 mg/ml 50–150 μm DBM (DBM) for 2 days. Alkaline phosphatase (ALP) activity (nmoles p-Nitrophenol/h) was determined and normalized to DNA (μg). Error bars indicate + 1 standard deviation from the mean (n=5). Bars connected with horizontal lines with the * symbol are significantly different ($p<0.05$).

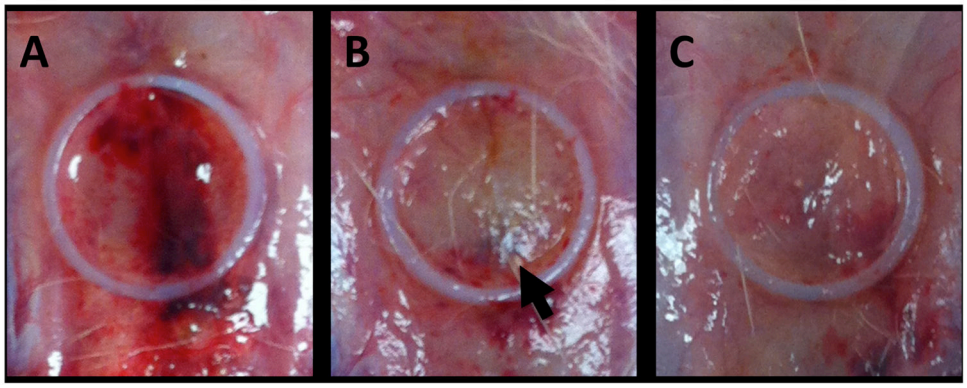

Figure 6.

Gross images taken at specimen harvest after dissection of soft tissue showing representative samples from the empty (A), 1:1 (B), and 3:1 (C) groups. Images show the transverse plane viewed from directly above. The Teflon ring is visible in white. The black arrow indicates the circular edge of an intact disc shaped construct.

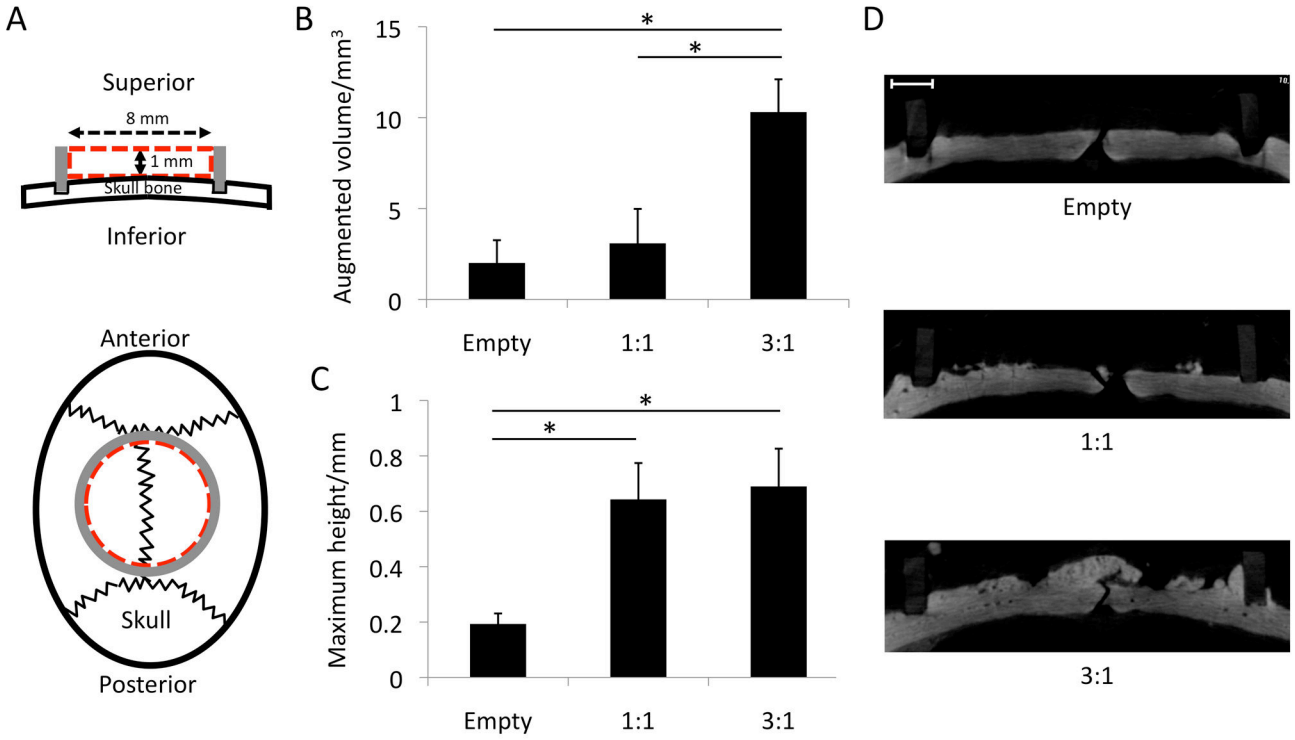

Figure 7.

Coronal and transverse schematic views of the surgical setup for the augmentation procedure (A), augmented bone volume in the region of interest (B), maximum height of new bone in the region of interest measured from the native bone surface (C), and representative raw μCT images showing mineralized tissue in the coronal plane (D). Error bars indicate + 1 standard deviation from the mean (n=8). Bars connected with horizontal lines with the * symbol are significantly different ($p<0.05$). The red dashed line indicates the region of interest in (A). The groove drilled for ring placement is visible at the lateral edges of each image in (D). The scale bar in (D) represents 1 mm.

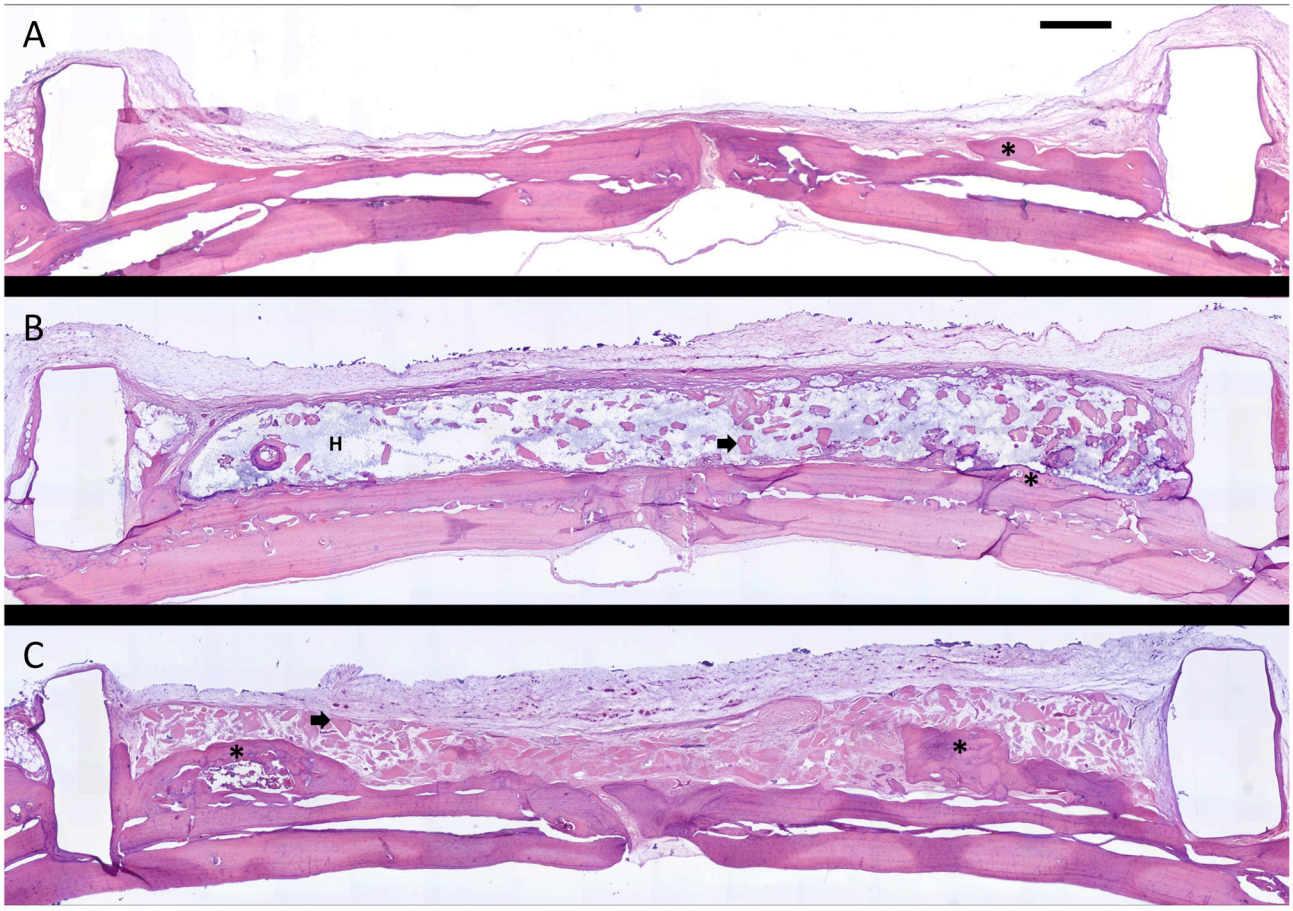

Figure 8.

Representative coronal H&E stained histological sections from the empty (A), 1:1 (B), and 3:1 (C) groups (original magnification 10x). The scale bar indicates 0.5 mm. Augmented bone is indicated by the *, DBM particles by arrows, and the OPF hydrogel is labeled “H”.

Table 1

IN VITRO

	DBM:OPF[a]	Particle size (μm)	Media
	1:3	50–150/150–250	PBS/Col PBS[b]
	1:1	50–150/150–250	PBS/Col PBS
	3:1	50–150/150–250	PBS

IN VIVO

	DBM:OPF	Particle size (μm)	
1:1	1:1	50–150	
3:1	3:1	50–150	
Empty	N/A	N/A	

[a] DBM:OPF refers to the ratio of the components on a dry weight basis

[b] Col PBS refers to PBS supplemented with 400 ng/ml collagenase 1A